

## Superior oxygen and glucose supply in perfusion cell cultures compared to static cell cultures demonstrated by simulations using the finite element method

Shinji Sugiura,<sup>1</sup> Yusuke Sakai,<sup>2</sup> Kohji Nakazawa,<sup>2</sup> and Toshiyuki Kanamori<sup>1,a)</sup>

<sup>1</sup>*Drug Assay Device Team, Research Center for Stem Cell Engineering, National Institute of Advanced Industrial Science and Technology (AIST), Central 5, 1-1-1 Higashi, Tsukuba, Ibaraki 305-8565, Japan*

<sup>2</sup>*Department of Life and Environment Engineering, The University of Kitakyushu, 1-1 Hibikino, Wakamatsu-ku, Kitakyushu, Fukuoka 808-0135, Japan*

(Received 15 February 2011; accepted 21 April 2011; published online 29 June 2011)

Oxygen and glucose supply is one of the important factors for the growth and viability of the cells in cultivation of tissues, e.g., spheroid, multilayered cells, and three-dimensional tissue construct. In this study, we used finite element methods to simulate the flow profile as well as oxygen and glucose supply to the multilayered cells in a microwell array chip for static and perfusion cultures. The simulation results indicated that oxygen supply is more crucial than glucose supply in both static and perfusion cultures, and that the oxygen supply through the wall of the perfusion culture chip is important in perfusion cultures. Glucose concentrations decline with time in static cultures, whereas they can be maintained at a constant level over time in perfusion cultures. The simulation of perfusion cultures indicated that the important parameters for glucose supply are the flow rate of the perfusion medium and the length of the cell culture chamber. In a perfusion culture chip made of oxygen-permeable materials, e.g., polydimethylsiloxane, oxygen is hardly supplied via the perfusion medium, but mainly supplied through the walls of the perfusion culture chip. The simulation of perfusion cultures indicated that the important parameters for oxygen supply are the thickness of the flow channel and the oxygen permeability of the walls of the channel, i.e., the type of material and the thickness of the wall. © 2011 American Institute of Physics.

[doi:10.1063/1.3589910]

### I. INTRODUCTION

The cell-based assay is an important analytical method in drug discovery.<sup>1,2</sup> However, one of the drawbacks of conventional cell-based assays in the drug discovery is the lowered function of the cells in comparison to cells *in vivo*. To overcome this drawback, the use of microprocesses, e.g., microfabrication,<sup>3-5</sup> microfluidics,<sup>6-8</sup> and micropatterning,<sup>9-11</sup> is on the rise, and the microprocesses are making it easier to precisely control the “cell culture environment.”<sup>12,13</sup>

Recently, we and other research groups have developed the perfusion culture microchamber array chips<sup>6-8</sup> and have applied the perfusion culture microchamber array chips to drug toxicity testing.<sup>14</sup> In the perfusion cultures on microchips, the growth and morphology of the cells were affected by the flow rate of the perfusion medium.<sup>6,14</sup> On the other hand, in the static culture, Nakazawa *et al.* also found that the spheroids in the central area of the microwell array were

<sup>a)</sup> Author to whom correspondence should be addressed. Electronic mail: t.kanamori@aist.go.jp.

smaller than that in the periphery area (data not shown). These results indicate that the oxygen and glucose supply is important for the cell growth and cell viability for the perfusion culture in the microchamber array and static spheroid culture in the microwell array.

Generally, most of the microfluidic cell culture chips in the previous studies are made of polydimethylsiloxane (PDMS), which has high gas permeability.<sup>15</sup> The high gas permeability potentially enables the oxygen supply through the wall of the chips. Rates of oxygen and glucose supply in a microchamber and microwell on a chip can be formulated by using normal-reaction diffusion equations.<sup>16</sup> Sumaru *et al.*<sup>17</sup> reported that the oxygen supply, rather than glucose supply, is critical for cell culture in microchips. Based on this finding, we hypothesized that oxygen supply is critical in perfusion culture in the microchamber array and static spheroid culture in the microwell array, and that oxygen supply to the cells grown in a static culture is potentially poorer than that in a perfusion microchamber.

However, it is practically impossible to solve the equations that have been derived for an actual microchamber and a microwell on a chip. In this study, we studied the complex reaction diffusion phenomena by using the finite element method (FEM). We compared oxygen and glucose supply to multilayered cells in a microwell array chip for static and perfusion cultures, and confirmed superior supply of both oxygen and glucose in the perfusion culture.

## II. MODELS FOR FEM

In this study, we assumed that 1024 ( $32 \times 32$ ) microwells ( $300 \mu\text{m}$  in diameter and depth) were arrayed in a reticular pattern at a pitch of  $330 \mu\text{m}$  on a plane, similar to that used by Nakazawa and colleagues.<sup>3-5</sup> We used a commercially available FEM software, COMSOL MULTIPHYSICS version 3.5a (COMSOL; Burlington, MA), to make a three-dimensional model of the microwell array chip and to calculate velocity and concentration profiles in the models.

### A. Model for static culture

We assumed that the microwells described above were arrayed at the center of the bottom of a 35 mm diameter Petri dish. To reduce the memory and calculation load of the computer, we made a model of one-eighth part of the Petri dish (Fig. 1) considering the symmetry of the circular Petri dish and the square-shaped microwell array. Based on the aforementioned experiments,<sup>3-5</sup> the depth of the cell culture medium was assumed to be 2 mm and cells seeded into the microwells were assumed to form layers that were  $92.1 \mu\text{m}$  thick at the bottom of the microwells. The thickness was calculated by assuming that the cell density was  $1.5 \times 10^{14}$  cells/ $\text{m}^3$  and that  $1 \times 10^6$  cells were seeded into all of the 1024 microwells. The thickness of the cell layer corresponds to the five cell layers.

### B. Model for perfusion culture

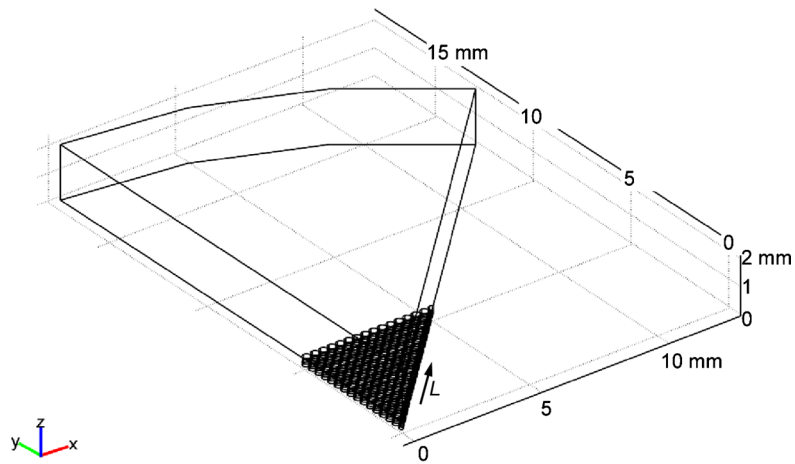
We assumed that the microwells described above were arrayed at the bottom of a parallel flow channel that was  $500 \mu\text{m}$  thick. To reduce the memory and calculation load of the computer, we made a model of half of one line of the microwells (Fig. 2). The layer of the seeded cells was assumed to be the same as that described in Sec. II A.

### C. Calculations

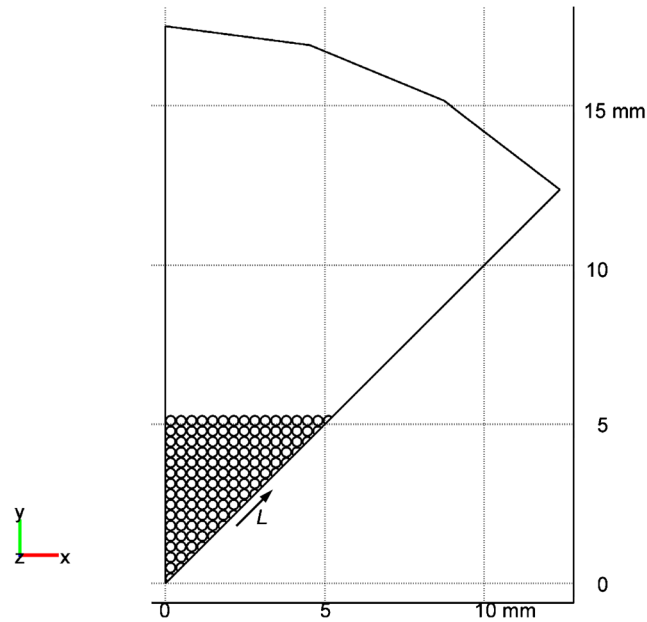
The flow velocity profile in the perfusion culture model was calculated with the Navier–Stokes equations. The viscosity and density of the medium were assumed to be the same as those of water at 310 K. The medium was assumed to be fed from the inlet [the far left square in Fig. 2(a)] at a uniform velocity. Any flow of the medium was not considered in the static culture model.

The concentration profiles for both the static and the perfusion culture models were calculated with a normal-reaction diffusion equation as follows:

(a)



(b)



(c)

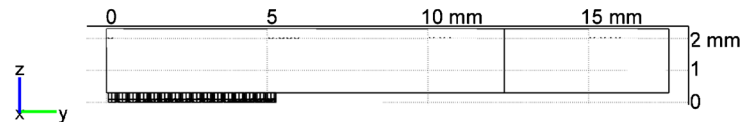


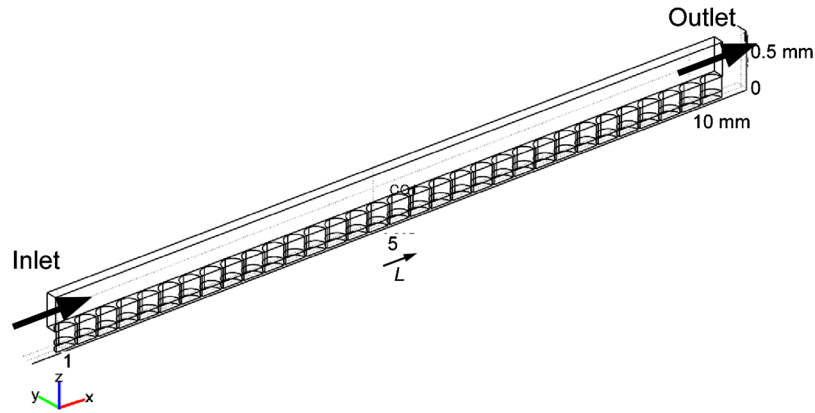
FIG. 1. Geometric model for the static culture: (a) perspective view and (b) top view.

$$\frac{\partial C}{\partial t} = \nabla(-D \nabla C) - R, \quad (1)$$

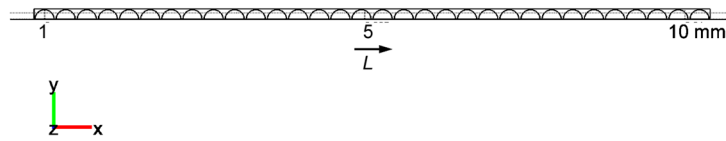
where  $C$  denotes the concentration ( $\text{mol}/\text{m}^3$ ),  $t$  is the time (seconds), and  $D$  is the diffusion coefficient ( $\text{m}^2/\text{s}$ ).  $R$  denotes the consumption rate ( $\text{mol}/\text{m}^3 \text{ s}$ ), which was zero in the medium.

The value of  $R$  was assumed to follow the Michaelis–Menten kinetics:

(a)



(b)



(c)

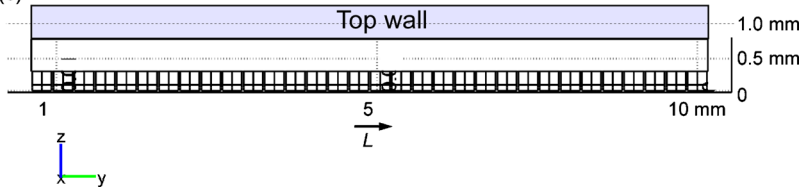


FIG. 2. Geometric model for the perfusion culture: (a) perspective view and (b) top view.

$$R = \frac{V_{\max} C}{K_h + C}, \quad (2)$$

where  $V_{\max}$  denotes the maximal consumption rate ( $\text{mol}/\text{m}^3 \text{ s}$ ) and  $K_h$  is the Michaelis constant ( $\text{mol}/\text{m}^3$ ).

In this study, we focused on the concentration profiles for oxygen and glucose because these are the essential factors in cell culture. We assumed the  $D$  values for oxygen and glucose in the medium and cell layer are the same values as those of water at 310 K and estimated them to be  $2.10 \times 10^{-9}$  and  $9.91 \times 10^{-10}$   $\text{m}^2/\text{s}$  for oxygen and glucose, respectively. The values of  $V_{\max}$  and  $K_h$  for oxygen consumption by rat primary hepatocytes were found to be  $2.0 \times 10^{-16}$   $\text{mol}/\text{s cell}$  and  $4.05 \times 10^{-3}$   $\text{mol}/\text{m}^3$ , respectively, based on the data obtained by Foy *et al.*<sup>18</sup> Not finding any values in literature, we estimated the  $V_{\max}$  and  $K_h$  values for glucose in the microwells to be one-sixth of the corresponding values for oxygen because aerobic respiration consumes 6 moles of oxygen per mole of glucose.

The mode of mesh generation for a model generally affects the results obtained by FEM. In this study, the mesh was generated by the automatic mode of COMSOL and the total number of tetrahedral elements was 139 160 for the static culture model and 53 640 for the perfusion model.

To reduce the computational load and memory, the velocity profile at a steady state was first calculated, and the concentration profile was then calculated for oxygen or glucose by using the predetermined velocity profile.

### III. RESULTS AND DISCUSSION

#### A. Static culture

We calculated time-dependent concentration profiles in the static culture model shown in Fig. 1 by assuming that the oxygen concentration in the uppermost layer of the medium was constant at  $0.192 \text{ mol/m}^3$ ; this value is the oxygen concentration in water that has been equilibrated with air containing saturated water vapor and 5% carbon dioxide at 310 K. The initial oxygen concentration in the medium and the cell layer was  $0.192 \text{ mol/m}^3$ , also. The initial glucose concentration in the medium and the cell layer was  $5.56 \text{ mol/m}^3$ , assuming that Eagle's minimal essential medium was used.

It is well known that diffusion reaches a pseudosteady state at a time (seconds) of  $l^2/D$ , where  $l$  is the diffusion distance (meters).<sup>19</sup> As the diffusion of oxygen and glucose was relatively fast compared to the consumption of oxygen and glucose by the cells, we assumed that the consumption of oxygen and glucose would not affect their concentration profiles in a pseudosteady state. Therefore, the concentrations for these two factors were assumed to reach a pseudosteady state at  $l^2/D$ . Here,  $l^2/D$  was 1900 s for oxygen and 4040 s for glucose, assuming that  $l$  is 2 mm, which is the thickness of the medium.

Generally, the oxygen concentration reaches a steady state, wherein the rate of oxygen supply through the surface of the medium is equal to the rate of oxygen consumption by the cells. As seen from the model shown in Fig. 1, the oxygen concentration profiles at the surface of the cell layers, aligned at  $45^\circ$  in the microwells, were calculated every second for 1900/4, 1900/2, and 1900 s, as shown in Fig. 3(a). The  $C_s$  values denote the concentration of oxygen or glucose at the surface of the cell layers and  $L$  is the distance (meters) from the center to the corner of the chip. Figure 3(a) indicates that the oxygen concentration almost achieved a steady state at 1900 s.

The glucose concentrations obtained at the same points and at 4040 s and  $10 \times 4040$  s are shown in Fig. 3(b). The glucose concentration almost achieved a pseudosteady state at 4040 s (data not shown) and gradually decreased after achieving a pseudosteady state because of the glucose consumption by the cultured cells. Generally, the static culture requires medium exchange every 1–3 days due to this gradual glucose consumption and glucose concentration changes through this culture period.

The glucose concentration was much higher than  $K_h$  ( $6.75 \times 10^{-4} \text{ mol/m}^3$ ) even in the central region of the chip, and the result indicates adequately high glucose concentration for multilayer cell culture. On the other hand, oxygen concentration in this region was lower than  $K_h$  ( $4.05 \times 10^{-3} \text{ mol/m}^3$ ), suggesting that it was very difficult to maintain aerobic respiration in the deeper levels of the cell layer in the central area of the microwell array. Indeed, oxygen concentration did not remain enough high even in the peripheral region of the microwells. These results reveal that oxygen supply is a more crucial factor for cell culture than glucose supply.<sup>17</sup>

#### B. Perfusion culture

In the perfusion culture model shown in Fig. 2, time-dependent concentration profiles were calculated for oxygen and glucose every 2 s until the average retention times of the perfusion medium for three different inlet velocities. The retention times were 1056 s for the inlet velocity of  $1 \times 10^{-5} \text{ m/s}$ , 10 560 s for  $1 \times 10^{-6} \text{ m/s}$ , and 105 600 s for  $1 \times 10^{-7} \text{ m/s}$ . The initial concentration of oxygen in the flow channel and cell layer, and that in the medium fed into the flow channel, was  $0.192 \text{ mol/m}^3$ , and that of glucose was  $5.56 \text{ mol/m}^3$ ; these values are the same value we used for the static culture.

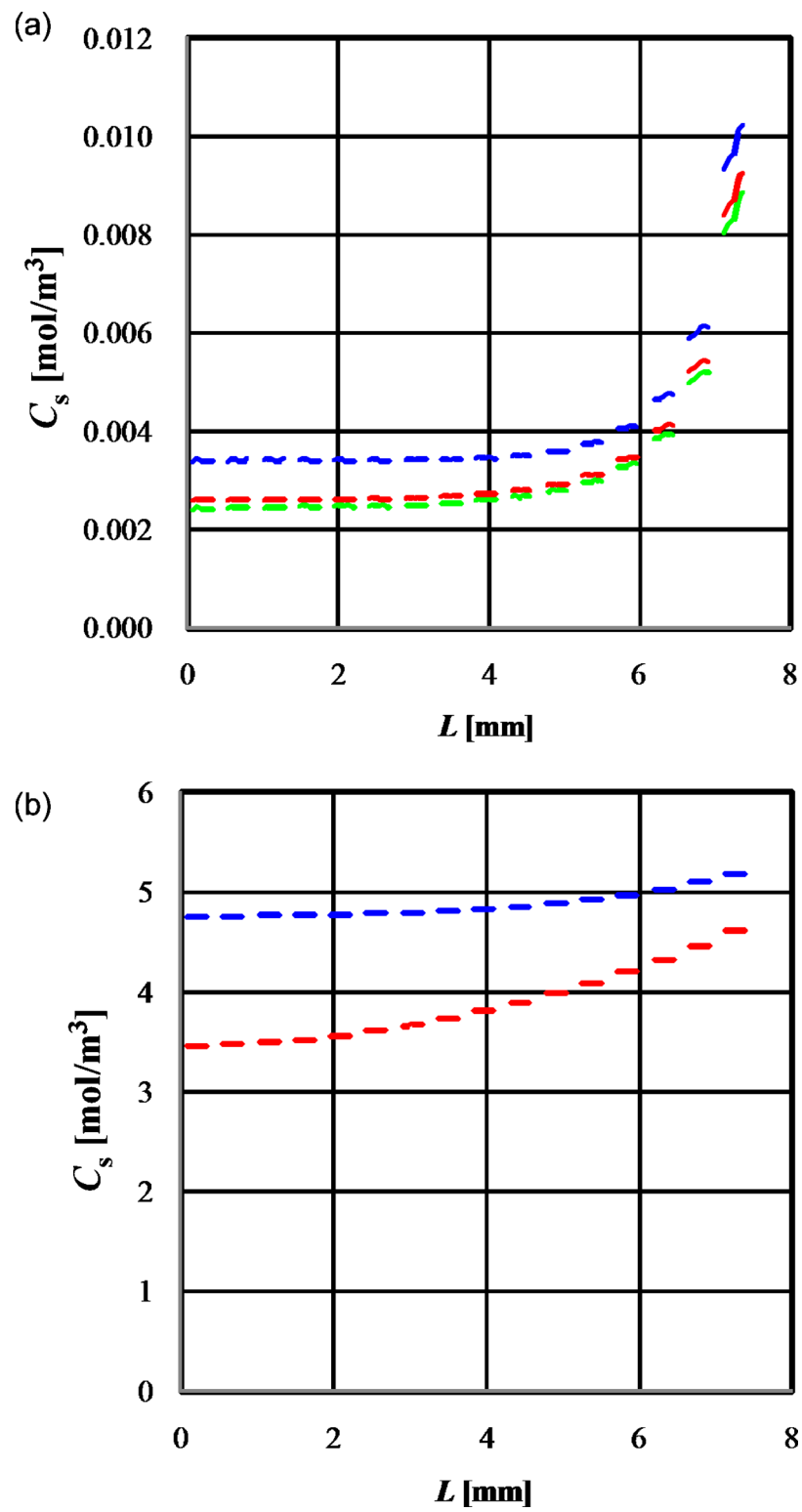


FIG. 3. Concentration profiles at the surface of the cell layers aligned at 45° in the microwells as per the static culture model shown in Fig. 1. (a) Oxygen concentration at 1900/4, 1900/2, and 1900 s for blue, red, and green lines, respectively. (b) Glucose concentration at 4040 s and 10×4040 s for blue and red line, respectively.

Figures 4(a) and 4(b) show the glucose concentration profiles at the surface of the cell layers in the microwells at  $l^2/D$  and the retention time, respectively. Figure 4(c) shows the glucose concentration profile at the  $x$ - $z$  plane shown in Fig. 2. The value of  $L$  denotes the distance (meters) from the inlet of the flow channel. Except for the result obtained with the velocity of  $1 \times 10^{-5}$  m/s, the overall glucose concentrations shown in Fig. 4(b) were less than that obtained for the static culture shown in Fig. 3(b). Especially, the glucose concentration drastically decreased at the downstream area in the case of low flow velocity. This phenomenon probably explains the effect of the flow rate of perfusion medium observed in the previous studies.<sup>6,14</sup> However, except for the result obtained with a velocity of  $1 \times 10^{-7}$  m/s, the overall glucose concentration remained higher than the  $K_h$  ( $6.75 \times 10^{-4}$  mol/m<sup>3</sup>) throughout the flow microchannel. In addition, the glucose concentration obtained for the static culture decreased with increasing culture time as shown in Fig. 3(b), whereas the glucose concentration was maintained at a constant level in the perfusion culture wherein cells were being continuously cultured under flowing medium with an appropriate flow rate. This is one of the advantages of perfusion culture.

Figure 5(a) shows the oxygen concentration profiles at the surface of the cell layers in the microwells composed of oxygen-impermeable wall at the retention time. The oxygen concentration shown in Fig. 5(a) was much lower in most of the area of the microwells, even at the highest perfusion flow rate, than that of the oxygen concentration in static cultures shown in Fig. 3(a). The practical perfusion culture chips were often made of PDMS<sup>6-8</sup> and are known for high oxygen permeability. The oxygen flux,  $J_s$  (mol/m<sup>2</sup> s), through a wall made of PDMS with a thickness,  $\delta$  (meters), can be calculated as follows:

$$J_s = \frac{D_w \alpha_w}{\delta} \left( P_a - \frac{C_m}{\alpha_m} \right), \quad (3)$$

where  $D_w$  denotes the diffusion coefficient (m<sup>2</sup>/s) of oxygen in PDMS,  $\alpha_w$  and  $\alpha_m$  are the sorption coefficients (mol/m<sup>3</sup> mm Hg) of oxygen into PDMS and water, respectively,  $P_a$  is the partial oxygen pressure (mm Hg) at the outer surface of the PDMS wall, and  $C_m$  is the oxygen concentration (mol/m<sup>3</sup>) at the inner surface of the PDMS wall.

Assuming that the top wall of the flow channel shown in Fig. 2(a) was made of PDMS and its thickness was 500  $\mu$ m,  $P_a$ ,  $D_w$ ,  $\alpha_w$ , and  $\alpha_m$  were found to be 142 mm Hg,  $3.4 \times 10^{-9}$  m<sup>2</sup>/s,  $1.35 \times 10^{-3}$  mol/m<sup>3</sup> mm Hg, and  $1.06 \times 10^{-2}$  mol/m<sup>3</sup> mm Hg, respectively. The oxygen concentration at the surface of the cell layers in the microwells was calculated at the corresponding retention times [Fig. 5(b)]. With increasing  $L$ , the oxygen concentration became constant at about 0.008 mol/m<sup>3</sup>, which is much higher than that obtained for the static culture and is higher than the  $K_h$  values for oxygen,  $4.05 \times 10^{-3}$  mol/m<sup>3</sup>. Figure 5(c) shows the oxygen concentration profile at the  $x$ - $z$  plane shown in Fig. 2. The concentration gradient was formed in the direction of the  $z$ -axis and the gradient was driving force for oxygen transfer.

These results reveal that oxygen supply through the PDMS wall is very crucial even in perfusion cultures, as discussed in the previous paper.<sup>17</sup> Provin *et al.*<sup>20</sup> also pointed out the importance of oxygen supply through the gas permeable wall based on their experimental results, in which high-density-cultured HepG2 cells in the perfusion culture exhibited the low oxygen consumption. Mehta *et al.*<sup>21</sup> also reported that the flow rate of the media does not significantly affect the oxygen uptake by cells in the PDMS microfluidic perfusion culture chip, of which the result is consistent with our calculated results.

In the case of the perfusion culture chips with PDMS wall, the maximal oxygen flux through a PDMS wall can be calculated by using Eq. (3) at  $C_m=0$ , which we can imagine in the case of a very high diffusion coefficient or a very thin flow channel and a very high consumption rate. Therefore, the maximal rate of oxygen supply through a PDMS wall is equal to  $D_w \alpha_w P_a A_t / \delta$ , where  $A_t$  is the area (m<sup>2</sup>) of the top wall of the flow channel. As  $P_a$  can be converted to concentration in the equation,  $C_a = \alpha_m P_a$ , the maximal oxygen supply rate through a PDMS wall is  $D_w \alpha_w C_a A_t / \alpha_m \delta$ . On the other hand, the maximal rate of oxygen supply in the perfusion medium is  $U_i A_i C_i$ , where  $U_i$  denotes the uniform flow velocity (m/s) at the inlet of the channel,  $A_i$  denotes the area of the inlet (m<sup>2</sup>), and  $C_i$  denotes the oxygen concentration (mol/m<sup>3</sup>) at the inlet.

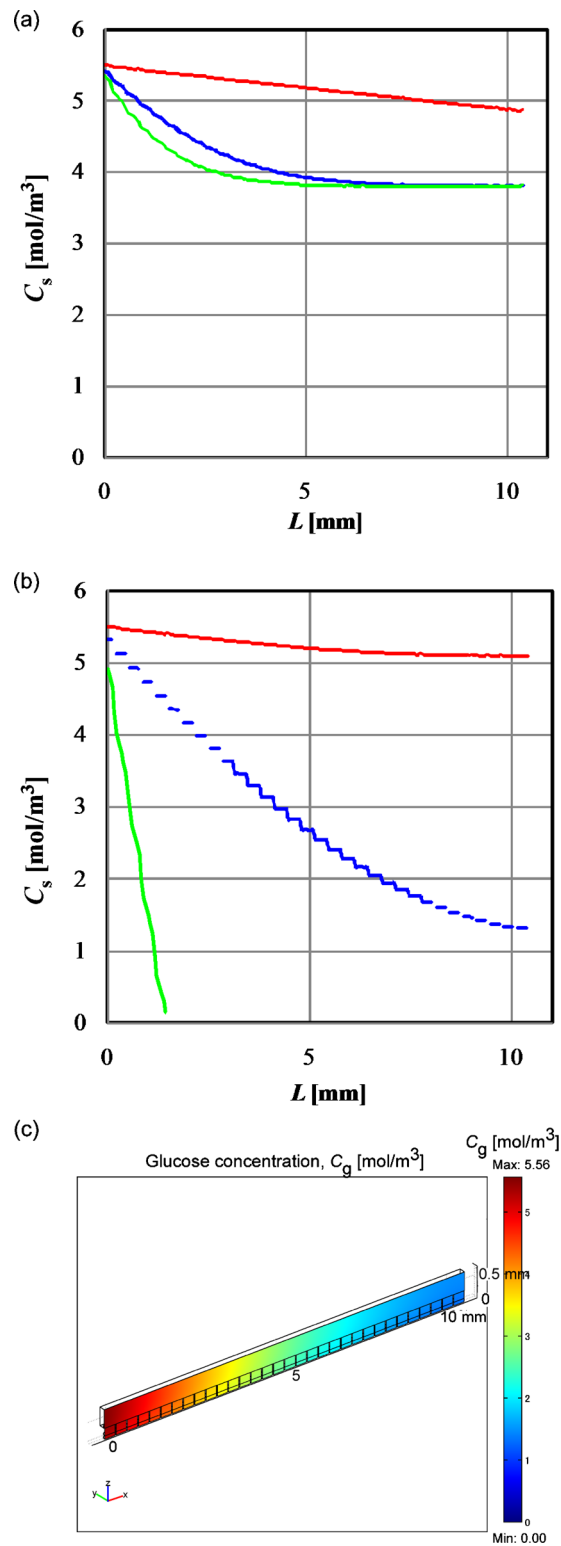


FIG. 4. Glucose concentration profiles in the microwells in the perfusion culture model shown in Fig. 2. (a) Glucose concentration at the surface of the cell layers at 4040 s. The inlet velocities of the medium are  $1 \times 10^{-5}$ ,  $1 \times 10^{-6}$ , and  $1 \times 10^{-7}$  m/s for red, blue, and green lines, respectively. (b) Glucose concentration profile at the surface of the cell layers at retention time. The inlet velocities of the medium and retention times are  $1 \times 10^{-5}$  m/s and 1056 s,  $1 \times 10^{-6}$  m/s and 10 560 s, and  $1 \times 10^{-7}$  m/s and 105 600 s for red, blue, and green lines, respectively. (c) Glucose concentration profile at the  $x$ - $z$  plane with  $1 \times 10^{-6}$  m/s inlet velocity at 10 560 s.



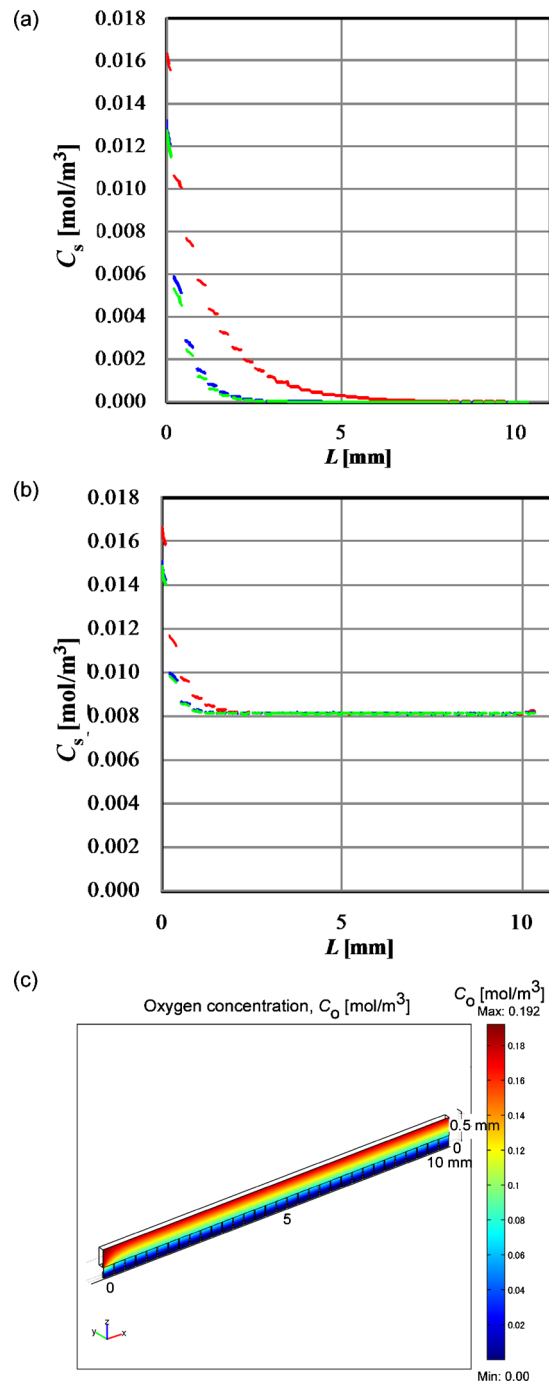


FIG. 5. Oxygen concentration profiles at the average retention time in the microwells in the perfusion culture model shown in Fig. 2. (a) Oxygen concentration at the surface of the cell layers oxygen-impermeable top wall. The inlet velocities of the medium are  $1 \times 10^{-5}$ ,  $1 \times 10^{-6}$ , and  $1 \times 10^{-7}$  m/s for red, blue, and green lines, respectively. (b) Oxygen concentration profile in the microwells with oxygen-permeable top wall. The inlet velocities of the medium are  $1 \times 10^{-5}$ ,  $1 \times 10^{-6}$ , and  $1 \times 10^{-7}$  m/s for red, blue, and green lines, respectively. (c) Oxygen concentration profile in the microwells with oxygen-permeable top wall at the  $x$ - $z$  plane with  $1 \times 10^{-6}$  m/s inlet velocity at 10 560 s.

In the case discussed here, because  $C_a = C_i$ , the ratio of the maximal rate of oxygen supply in the perfusion medium to the maximal rate of oxygen supply through the PDMS wall is  $U_i \delta \alpha_m A_i / D_w \alpha_w A_t$ , which is  $8.87 \times 10^2 U_i$ . As the maximal practical value of  $U_i$  is  $1 \times 10^{-5}$  m/s,

we can expect that oxygen must be supplied mainly through the PDMS wall. This result means that a thinner channel and PDMS wall are necessary to maintain multilayer cell culture on a chip, even if the chip is equipped with a medium perfusion feature.

#### IV. SUMMARY AND CONCLUSIONS

Even in a simple monolayer cell culture system, we can estimate the temporal-spatial changes of velocity, concentration, and temperature with partial differential equations based on transport phenomena. However, it is very difficult to solve the equations because of the complex boundary conditions. Recently, microprocess has been attracting attention in order to better handle and culture animal cells, which are increasingly used in pharmaceutical and medical areas. However, it is not easy to measure physical conditions such as velocity, concentration, and temperature in a microchamber and microwell during cell handling and culture. In this study, therefore, we explored the advantages of perfusion culture over static culture for a microwell array chip by calculating the temporal-spatial changes of oxygen and glucose concentrations in microwell array on chips. Multilayered cells were cultivated in these microwell arrays by using a commercially available FEM application, which has been made more feasible due to significant advances in the calculation power of a personal computer.

The following results were obtained:

- (1) The concentrations of oxygen and glucose in a static culture of multilayered cells inside a microwell array chip are lower in the central region than that in the peripheral region. Therefore, aerobic respiration is impossible in the central region of the chip, where the oxygen concentration is lower than the Michaelis constant.
- (2) Glucose concentrations can be maintained at a constant level over time in perfusion cultures, whereas they decline with time in static cultures. The glucose concentration in a perfusion culture chip decreases with increasing distance from the inlet of the cell culture chamber. Also, the concentration profile of glucose in the cell culture chamber changes substantially with the flow rate of the medium.
- (3) In a perfusion culture chip, oxygen is hardly supplied via the perfusion medium, but mainly supplied through the walls of the cell culture chamber.

The above results suggest that the design of a perfusion culture chip should take the following into account:

- (1) the flow rate of the perfusion medium and the length of the cell culture chamber with respect to glucose supply, and
- (2) the thickness of the flow channel and the oxygen permeability of the walls of the channel with respect to oxygen supply.

#### ACKNOWLEDGMENTS

This work was supported by MEXT KAKENHI (Grant No. 22760618).

- <sup>1</sup>M. Y. Lee and J. S. Dordick, *Curr. Opin. Biotechnol.* **17**, 619 (2006).
- <sup>2</sup>J. Hüser, *High-Throughput Screening in Drug Discovery* (Wiley-VCH, Hoboken, 2006), Vol. 35.
- <sup>3</sup>J. Fukuda and K. Nakazawa, *Tissue Eng.* **11**, 1254 (2005).
- <sup>4</sup>J. Fukuda, Y. Sakai, and K. Nakazawa, *Biomaterials* **27**, 1061 (2006).
- <sup>5</sup>Y. Sakai, S. Yamagami, and K. Nakazawa, *Cells Tissues Organs* **191**, 281 (2010).
- <sup>6</sup>L. Kim, M. D. Vahey, H. Y. Lee, and J. Voldman, *Lab Chip* **6**, 394 (2006).
- <sup>7</sup>S. Sugiura, J. Edahiro, K. Kikuchi, K. Sumaru, and T. Kanamori, *Biotechnol. Bioeng.* **100**, 1156 (2008).
- <sup>8</sup>P. J. Hung, P. J. Lee, P. Sabounchi, R. Lin, and L. P. Lee, *Biotechnol. Bioeng.* **89**, 1 (2005).
- <sup>9</sup>S. R. Khetani and S. N. Bhatia, *Nat. Biotechnol.* **26**, 120 (2008).
- <sup>10</sup>J. Fukuda, A. Khademhosseini, Y. Yeo, X. Yang, J. Yeh, G. Eng, J. Blumling, C.-F. Wang, D. S. Kohane, and R. Langer, *Biomaterials* **27**, 5259 (2006).
- <sup>11</sup>K. Kikuchi, K. Sumaru, J. Edahiro, Y. Ooshima, S. Sugiura, T. Takagi, and T. Kanamori, *Biotechnol. Bioeng.* **103**, 552 (2009).
- <sup>12</sup>J. El-Ali, P. K. Sorger, and K. F. Jensen, *Nature (London)* **442**, 403 (2006).
- <sup>13</sup>L. F. Kang, B. G. Chung, R. Langer, and A. Khademhosseini, *Drug Discovery Today* **13**, 1 (2008).

- <sup>14</sup> S. Sugiura, K. Hattori, and T. Kanamori, *Anal. Chem.* **82**, 8278 (2010).
- <sup>15</sup> M. A. Eddings and B. K. Gale, *J. Micromech. Microeng.* **16**, 2396 (2006).
- <sup>16</sup> K. Sumaru and T. Kanamori, *Biochem. Eng. J.* **20**, 127 (2004).
- <sup>17</sup> K. Sumaru, S. Sugiura, and T. Kanamori, *Biochem. Eng. J.* **36**, 304 (2007).
- <sup>18</sup> B. D. Foy, A. Rotem, M. Toner, R. G. Tompkins, and M. L. Yarmush, *Cell Transplant* **3**, 515 (1994).
- <sup>19</sup> J. Crank, *The Mathematics of Diffusion* (Oxford University Press, New York, 1975).
- <sup>20</sup> C. Provin, K. Takano, T. Yoshida, Y. Sakai, T. Fujii, and R. Shirakashi, *Biomed. Microdevices* **11**, 485 (2009).
- <sup>21</sup> G. Mehta, K. Mehta, D. Sud, J. W. Song, T. Bersano-Begey, N. Futai, Y. S. Heo, M. A. Mycek, J. J. Linderman, and S. Takayama, *Biomed. Microdevices* **9**, 123 (2007).